Longitudinal shift in diabetic wound microbiota correlates with prolonged skin defense response

Elizabeth A. Grice[a], Evan S. Snitkin[a], Laura J. Yockey[a], Dustin M. Bermudez[b], NISC Comparative Sequencing Program[c,1], Kenneth W. Liechty[d,2], and Julia A. Segre[a,2]

[a]Genetics and Molecular Biology Branch and [c]National Institutes of Health Intramural Sequencing Center, National Human Genome Research Institute, Bethesda, MD 20892; [b]Department of Surgery, University of Pennsylvania School of Medicine, Philadelphia, PA 19104; and [d]Department of Surgery, University of Mississippi Medical Center, Jackson, MS 39216

Diabetics frequently suffer from chronic, nonhealing wounds. Although bacterial colonization and/or infection are generally acknowledged to negatively impact wound healing, the precise relationship between the microbial community and impaired wound healing remains unclear. Because the host cutaneous defense response is proposed to play a key role in modulating microbial colonization, we longitudinally examined the diabetic wound microbiome in tandem with host tissue gene expression. By sequencing 16S ribosomal RNA genes, we show that a longitudinal selective shift in wound microbiota coincides with impaired healing in diabetic mice (Lepr$^{db/db}$; db/db). We demonstrate a parallel shift in longitudinal gene expression that occurs in a cluster of genes related to the immune response. Further, we establish a correlation between relative abundance of *Staphylococcus* spp. and the expression of cutaneous defense response genes. Our data demonstrate that integrating two types of global datasets lends a better understanding to the dynamics governing host–microbe interactions.

wound healing | microbiome | innate immunity | diabetes | gene expression

Diabetes currently affects ≈24 million people in the United States, and this number is expected to at least double in the next 25 y, along with associated health care expenditures (1). One of the most common and costly complications of diabetes is chronic nonhealing wounds, affecting as many as 15% of diabetics and exceeding $1.5 billion in annual costs in the United States alone (2). It is widely appreciated that diabetic wounds do not follow the precisely orchestrated course of events observed in normal wound healing, consisting of phases of coagulation, inflammation, migration/proliferation, and remodeling. In addition to peripheral neuropathy and vasculopathy, increased bacterial colonization and/or infection of the diabetic wound have a deleterious effect on healing (3). Systemic antibiotics and dressings are often used to treat chronic wounds, but clinical outcome studies do not uniformly support the efficacy of such measures. A better understanding of the relationship between bacterial colonization and impaired wound healing is necessary to reevaluate therapeutic strategies.

Prevalent species isolated by culture-based methods from diabetic foot ulcers in humans include *Staphylococcus aureus*, *Staphylococcus epidermidis*, *Streptococcus* species, *Pseudomonas aeruginosa*, *Enterococcus* species, *Peptostreptococcus* species, *Bacteroides* species, and *Prevotella* species (4, 5). Culture-based assays inherently are biased toward the 1% of microbes that are able to thrive in isolation and in diagnostic growth conditions (6). We recently surveyed the resident microbiota of healthy human skin by using a less biased, culture-independent method of sequencing the highly conserved bacterial 16S ribosomal RNA gene (7). Many of those bacteria identified as commensals by our genomic analysis have also been cultured from diabetic wounds (4, 5).

The skin is the first line of defense to the external environment. The skin's ability to resist infection is likely a key factor in a microbe's transition from commensal to pathogenic (8). The keratinocytes that make up this barrier are a potent source of innate immune sentinels such as Toll-like receptors (TLRs) and Nod-like receptors (NLRs), and innate immune mediators such as antimicrobial peptides (AMPs), chemokines, and cytokines (9). As a result, the cutaneous defense response and the skin microbiome are likely to be highly interactive, maintaining a delicate balance between defending against infection and eliciting an excessive inflammatory response. Further, chronic inflammation has been implicated in the pathogenesis of nonhealing diabetic wounds (10–13). Necrotic tissue and low oxygen tension present in the wound encourage proliferation and colonization of microbes. High microbial burden could likely in part be responsible for eliciting an excessive inflammatory response and retarding wound closure.

We used a genetically diabetic mouse model, the Lepr$^{db/db}$ mouse deficient for the leptin receptor (db/db) (14), to examine this complex interaction. The db/db mouse exhibits many of the features of type 2 diabetes and the most severe and consistent impaired wound healing as compared with other diabetic animal models (15, 16). We performed 16S rRNA sequencing to longitudinally characterize the microbial community that colonizes diabetic skin and wounds. We then used longitudinal transcriptional profiling to demonstrate that the shift in microbiota corresponds to an aberrant host cutaneous defense response in diabetic skin and wounds.

Results

The db/db Skin Microbiome Varies Quantitatively and Qualitatively from the db/+ Skin Microbiome. To determine whether the total bacterial load colonizing the skin was similar in db/db and db/+ mice, we used a quantitative PCR strategy based on a small amplicon of the 16S rRNA gene (17, 18). One day before wounding (day −1), swabs of a 4-cm^2 area on the back of 10 mice of each genotype, db/db diabetic mice and db/+ healthy controls, were collected and DNA was extracted from the swabs. We calculated that on average 40 times more bacteria populated db/db skin as compared with db/+ skin ($P = 2.0 \times 10^{-4}$; Table S1).

To determine the baseline microbial diversity colonizing healthy and diabetic mouse skin, near-full-length 16S rRNA genes were sequenced from db/+ and db/db skin swabs ($n = 10$ mice of each genotype). These sequences were then assigned to the bacterial taxonomy as defined by the Ribosomal Database Project (19). On average, db/+ skin was colonized by the following bacterial phyla:

78.6 ± 4.0% Firmicutes, 14.9 ± 7.2% Proteobacteria, 2.4 ± 0.44% Actinobacteria, and 2.9 ± 0.82% Bacteroidetes. For further analysis, we focused on the 11 genera that comprise on average at least 1% of the total 16S sequences identified across all samples (Fig. 1). Within phylum Firmicutes, the genera *Staphylococcus* and *Aerococcus* were increased ($P = 0.005$ and 0.018, respectively), and *Streptococcus* and *Lachnospiraceae Incertae Sedis* were decreased ($P = 0.006$ and $P = 0.021$, respectively) in db/db skin as compared with db/+ skin. Within phylum Proteobacteria, an *Enterobacteriaceae*, most similar to *Klebsiella*, was increased ($P = 2.0 \times 10^{-4}$) and *Acinetobacter* was decreased ($P = 0.015$) in db/db skin as compared with db/+ skin. Within phylum Bacteroidetes, an unclassified *Porphyromonadaceae* was increased ($P = 0.02$) in db/db skin as compared with db/+ skin. Taken together, these data indicate that there is a quantitative and qualitative shift in bacterial species colonizing diabetic skin in the db/db mouse model.

Although our comparisons of relative abundance in this and following sections are at the genus level, the *Aerococcus, Klebsiella,* and *Weissella* genera we refer to were comprised at all time points exclusively of sequences corresponding to the species *A. viridans, K. oxytoca,* and *W. hellenica,* respectively. The genus *Staphylococcus* primarily consisted of *S. saprophyticus* with minor contribution from *S. epidermidis, S. capitis, S. lenti, S. auricularis, S. hominis, S. warneri,* and *S. cohnii.* When analyzed at the species level, the significance of the shift was driven by *S. saprophyticus,* with no other *Staphylococcus* species differing in frequency between groups at all time points. In the time points described below, when genera other than those discussed above consisted of mixed species, we indicate what those species are.

Impaired Healing of db/db Wounds Coincides with a Shift in Colonizing Bacteria. After characterizing the bacterial populations inhabiting unwounded mouse skin, we created a 6-mm full thickness excisional wound on the back of each mouse. These wounds were measured and photographed on days 3, 7, 14, 21, and 28 (Fig. 2 *A* and *B*). Wound size was determined by wound surface area measurement. Additionally, wounds were swabbed to capture bacteria on and under the eschar, and relative abundance of colonizing species was determined by sequencing 16S rRNA genes (Fig. 1).

On day 3 after wounding, db/+ wounds were on average 47.6% closed, whereas db/db wounds increased in size to an average of 132% of their original size ($P = 1.3 \times 10^{-9}$). Most db/db wounds were erythematous with mild exudate. Relative abundance of *Staphylococcus,* exclusively comprised of *S. saprophyticus* at this time point, was increased in both db/+ and db/db wounds as compared with day −1 unwounded skin. As compared with db/+ wounds, db/db wounds were characterized by increased *Aerococcus* ($P = 0.005$) and *Weissella* ($P = 0.002$) and decreased *Lachnospiraceae Incertae Sedis* ($P = 0.045$).

On day 7, db/+ wounds were 67.3% closed, whereas db/db wounds returned to their original size ($P = 2.9 \times 10^{-9}$). Erythema and mild exudate were still apparent in db/db wounds. Both db/db

and db/+ wounds were still colonized by a majority of *Staphylococcus* but significantly greater *Lachnospiraceae Incertae Sedis,* unclassified *Lachnospiraceae, Streptococcus* (consisting of *S. oralis, S. sanguinis, S. thermophilus,* and *S. mitis*), and *Enterococcus* (consisting of species *E. faecalis* and *E. gallinarium*) colonized db/+ wounds as compared with db/db wounds ($P = 5.1 \times 10^{-4}$, 0.002, 0.006, 0.02, respectively). Other shifts included increased *Weissella* in db/db wounds as compared with db/+ wounds ($P = 0.02$).

By day 14, most db/+ wounds were completely reepithelialized, whereas db/db wounds were 58.6% closed ($P = 1.8 \times 10^{-13}$). Bacterial taxonomic differences between db/db and db/+ wounds were more pronounced. These differences included increased *Staphylococcus* and *Weissella* ($P = 0.05$ for both) and decreased *Lachnospiraceae Incertae Sedis,* unclassified *Lachnospiraceae, Streptococcus* (consisting of *S. mitis, S. sanguinis, S. oralis, S. thermophilus, S. S16-11,* and *S. F1*), and *Acinetobacter* (consisting of *A. lwoffi, A. johnsonii,* and *A. schindleri*) in db/db wounds as compared with db/+ wounds ($P = 1.1 \times 10^{-4}$, 1.3×10^{-4}, 7.5×10^{-4}, 0.002, respectively).

On day 21, db/db wounds were still open and grossly appeared to be hyperkeratotic. Bacteria colonizing db/db wounds was characterized by increased *Staphylococcus, Aerococcus,* and *Weissella* ($P = 0.01$, 0.03, 0.01, respectively), and decreased *Streptococcus* (consisting of *S. oralis, S. mitis, S. sanguinis, S. salivarius,* and *S. infantis*), *Acinetobacter* (consisting of *A. junii* and *A. LR30*), *Lachnospiraceae Incertae Sedis,* and unclassified *Lachnospiraceae* as compared with db/+ wounds ($P = 9.4 \times 10^{-4}$, 2.3×10^{-3}, 8.2×10^{-5}, 4.9×10^{-4}, respectively).

Although day 28 db/db wounds appeared to be completely reepithelialized, they still appeared to be grossly hyperkeratotic in the previously wounded area (Fig. 2 *A* and *B*). The db/db wound area was still colonized by an increased relative abundance of *Staphylococcus, Aerococcus,* and *Weissella* ($P = 0.02$, 1.8×10^{-4}, 2.3×10^{-4}, respectively) and decreased *Streptococcus* (consisting of *S. salivarius, S. oralis, S. 106–03c, S. thermophilus,* and *S. sanguinis*), *Lachnospiraceae Incertae Sedis,* unclassified *Lachnospiraceae,* and *Klebsiella* as compared with db/+ wounds ($P = 4.9 \times 10^{-3}$, 1.7×10^{-3}, 1.7×10^{-3}, 0.03, respectively).

To globally assess taxonomic diversity of bacteria colonizing wounds, we calculated the Shannon diversity index, which accounts for both richness and evenness of species (Fig. 3). We first clustered sequences into species-level operational taxonomic units (OTUs) of 99% sequence similarity by the furthest-neighbor method (20). At baseline on day −1, db/db skin was characterized by significantly decreased diversity of OTUs as compared with db/+ skin ($P = 0.007$). After wounding on day 3, both db/db and db/+ wounds were characterized by a significant decrease in overall bacterial diversity as compared with day −1 diversity ($P = 1.1 \times 10^{-4}$ and 0.024 respectively). OTU diversity of db/+ wounds then increased to become significantly greater than db/db diversity on day 7 ($P = 0.026$). The trend of decreased OTU diversity in db/db wounds as compared with db/+ wounds persisted through the
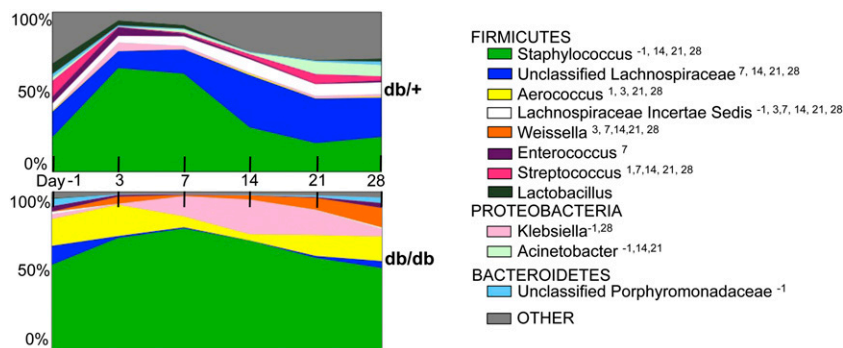
Fig. 1. Relative mean abundance of major bacterial genera at each time point in db/+ control mice and db/db diabetic mice ($n = 10$ mice of each genotype). *x* axis represents each time point in days. *y* axis is relative abundance (percentage) of bacterial genera. Superscripts on legend indicate day at which there is a statistically significant shift in that bacterial group (Mann–Whitney test; $P < 0.05$).
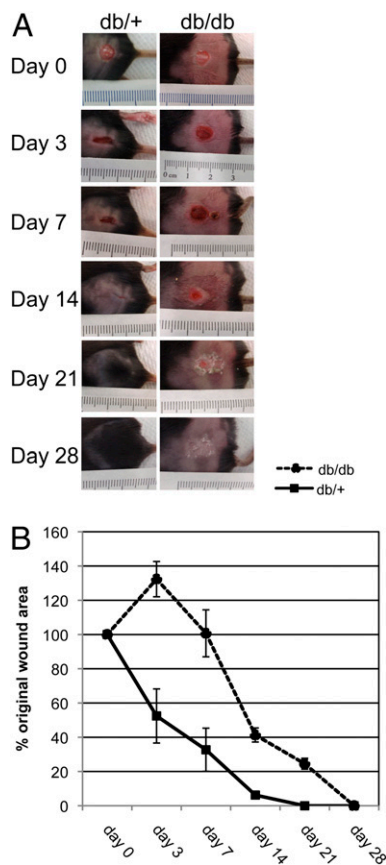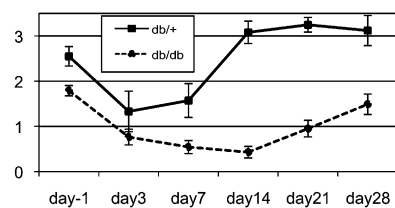
Fig. 2. Impaired wound healing phenotype in db/db mice. (*A*) Depicted is a 6-mm excisional wound as it heals over 28 d. The same db/+ and db/db mouse are depicted at each time point. (*B*) Average measurement of wound surface area over 28 d (*n* = 10 mice of each genotype). *y* axis represents percentage surface area of original 6-mm wound. Error bars represent SD of the mean. Wound size differences are significant (*P* < 0.05, Welch's *t* test) on days 3, 7, 14, and 21.


Fig. 3. Mean longitudinal microbiota diversity of db/+ and db/db mouse wounds as measured by the Shannon Diversity Index. Error bars represent SEM for *n* = 10 mice of each genotype. All time points are statistically significantly different between db/+ and db/db mice except for day 3 (*P* = 0.007, 0.026, 2.7×10^{-7}, 5.3×10^{-8}, and 0.001, respectively, by the Welch's *t* test).

entire time course (Fig. 3). We concluded that a distinct microbial population colonizes db/db wounds and is characterized by decreased diversity as compared with db/+ wounds.

Transcriptional Profiling Suggests Mobilized Immune Response in db/db Skin. Next, we sought to analyze the host tissue transcriptional response to wounding and how this response varied through the course of the healing process in db/+ and db/db mice. We first compared differential gene expression of unwounded db/db and db/+ skin (*n* = 4 mice of each genotype) to set a baseline for longitudinal transcriptional profiling. From the skin punch biopsies, we identified 1,487 differentially expressed transcripts, corresponding to 1,256 genes or ESTs, using a threshold of >1.5-fold change between db/db and db/+ transcripts at an adjusted *P* < 0.05. Of these genes and ESTs, 710 were up-regulated in db/db skin and 546 were down-regulated in db/db skin. Up-regulated transcripts in db/db skin were significantly enriched for those corresponding to Gene Ontology (GO) categories (21) of lipid metabolic process (59 genes, $P = 3.5 \times 10^{-9}$), vasculature development (22 genes, $P = 4.8 \times 10^{-3}$) and, notably, response to wounding (25 genes, *P* = 0.02). Down-regulated transcripts in db/db skin were enriched for the GO category developmental process (118 genes, $P = 1.5 \times 10^{-5}$).

Because we were primarily interested in differentially gene expression as part of the cutaneous defense response, we focused further analysis on genes falling within the partially overlapping GO categories immune response (IR), defense response (DR), and

response to wounding (WR) (Table S2). IR broadly encompasses any immune system response to a potential internal or invasive threat. DR specifically restricts damage or prevents infection when an organism is attacked by a foreign body or injured. WR captures changes in state or activity of an organism as a result of a stimulus suggesting damage to the organism (21). This subset of differentially expressed transcripts, corresponding to 68 genes, included those encoding members of the Toll-like receptor signaling pathways, complement and coagulation cascade, antimicrobial peptides, and acute phase inflammatory marker (Table S2). Kyoto Encyclopedia of Genes and Genomes (KEGG) analysis revealed that this subset of transcripts was significantly enriched for the complement and coagulation pathway (6 genes, *P* = 0.03). Unsupervised hierarchical clustering analysis of samples with respect to expression of all genes revealed a clear clustering pattern that separates db/db from db/+ skin (Fig. S1*A*). This same topology was preserved when clustering samples with respect to DR, IR, and WR genes (Fig. S1 *B, C, and D*, respectively).

These data indicated a distinct pattern of differential gene expression in db/db skin before wounding, including transcriptional mobilization of a subset of genes involved in IR, DR, and WR. Our findings support the relevance of further investigation of this response through the wound healing process.

Longitudinal Transcriptional Profile Analysis Reveals Prolonged Immune/Defense/Wounding Response. To longitudinally assess the host tissue response to wounding, wounds (*n* = 4 each db/db and db/+ at each time point) at days 3, 7, 14, and 21 were harvested. So as not to dilute effects at the wound edge, only 2 mm of tissue was collected at the wound margin. We chose to first obtain an overview of how similar db/db and db/+ wounds were to each other at each time point, especially pertaining to IR, DR, and WR genes. We performed unsupervised hierarchical clustering by using only IR, DR, or WR genes at all time points (Fig. 4*A* and Fig. S2). Trees built with respect to differential expression of IR, DR, and WR genes demonstrated similar topology. Specifically, day 0 gene expression of db/db and db/+ skin clustered closely together. Day 3 db/+ expression profiles were most similar to day 3 and 7 db/db expression profiles. Day 7 db/+ expression profiles were most similar to day 14 and 21 db/db expression profiles. These data suggested aberrant expression of IR, DR, and WR genes in the db/db wounds, specifically a delayed response compared with db/+ wounds.

To more stringently analyze and cluster our gene expression dataset, we used STEM (Short Time-series Expression Miner), a software program specifically designed to analyze longitudinal microarray gene expression data (22). STEM first generated model expression profiles with five time points to fit the data. After assigning each transcript to a profile, enrichment of genes in each profile was calculated to determine profile significance. STEM fit our dataset to 14 model expression profiles that were significantly enriched for transcripts expressed longitudinally in db/+ and db/db wounds. Two db/+ wound expression profiles were specifically enriched for transcripts belonging to GO categories IR, DR, and
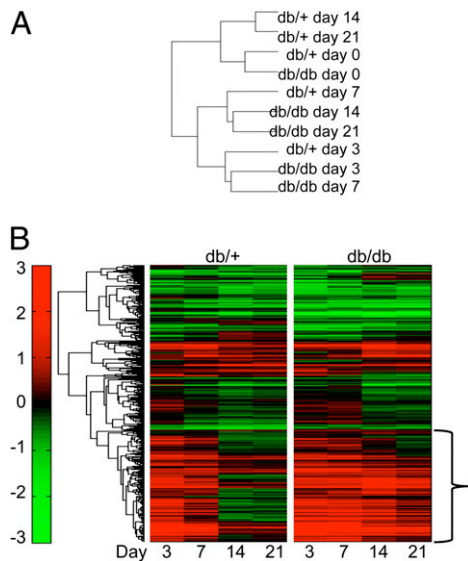
Fig. 4. Prolonged expression of genes corresponding to GO biological processes IR, DR, and WR. (*A*) Hierarchical cluster analysis of the 10 sample types (*n* = 4 mice of each genotype at five time points) with respect to IR genes. (*B*) The mRNA expression changes in IR, DR, and WR genes represented by a clustered heatmap. Red values indicate an increased expression relative to day 0, and green values indicate a decreased expression relative to day 0. A large subset of genes, indicated by the bracket, whose expression increases immediately in response to wounding in both db/+ and db/db mice shows an extended expression pattern in the db/db mice. These genes return to baseline expression levels by day 14 in db/+ wounds, but they do not return to baseline levels even at day 21 in db/db wounds.

WR. The behavior of these transcripts consisted of an initial spike at day 3 after wounding, followed by a decrease to baseline levels or lower. In db/db wounds, IR, DR, and WR transcripts were enriched among profiles characterized by an expression pattern that peaks on day 3 or day 7, but for the most part did not return to baseline levels during the time course we analyzed. Such transcripts represented 96 genes, and encode members of the TLR signaling pathways, cytokine and chemokine signaling pathways, acute inflammatory markers, and the complement cascade (Table S3). The prolonged pattern of expression of this subset of genes as identified by STEM was also apparent upon hierarchical clustering of all differentially expressed IR, DR, and WR genes (Fig. 4*B*).

We thus concluded that the majority of IR, DR, and WR transcripts were aberrantly expressed during the wound healing time course in db/db mice, reflecting a pattern of extended response. Our data are consistent with reported observations of persistent mRNA expression of the inflammatory cytokines IL-1β and TNFα and the chemokine MIP-1 in db/db wounds (23). Production of these cytokines and chemokines results in recruitment of macrophages, monocytes, and polymorphonuclear leukocytes, rich sources of reactive oxygen species (ROS), to the wound sites. ROS are not only responsible for direct to damage cellular components and structural proteins of the extracellular matrix, but also amplify signaling pathways responsible for the persistent inflammatory stage in chronic wounds (24).

Correlation of Selective Shift in Microbiome with Aberrant Expression of Cutaneous Defense Response Genes. Finally, we explored the possible association of the selective shifts in microbial diversity with the cutaneous transcriptional profiles of db/db and db/+ mice in response to wounding. We correlated the relative abundance of the 11 genera that comprise at least 1% of the total 16S sequences with relative gene expression levels. The nonparametric Spearman rank correlations of genera and the transcriptional profiles of IR,

DR, and RW genes are shown in Fig. S3. *Staphylococcus* is the only genus where IR, DR, and WR are enriched in correlations with $P <$ 0.01 (Fisher exact test, Benjamini-Hochberg corrected $P = 1.3 \times 10^{-5}$, 5.9×10^{-7}, 1.8×10^{-6}, respectively). To independently test this observation, we used a Gene Set Enrichment Analysis (GSEA) approach. Rather than considering only genes that achieve a correlation with a phenotype below a predetermined P value cutoff, GSEA instead searches for biological coherence among the entire set of correlations (25). Each of the 11 genera was tested independently by GSEA, assessing whether genes in IR, DR, and WR are enriched among those genes most positively or negatively (anti-) correlated with the relative abundance of the given genus. Again, *Staphylococcus* shows the most significant enrichment of IR, DR and WR genes among those most positively correlated in both db/+ and db/db mice ($P = 0.04$, 0.05, 0.02, respectively). The basis for this enrichment is clear, because *Staphylococcus* abundance increases immediately in response to wounding in both db/+ and db/db mice with a prolonged increase in db/db mice (Fig. 5 *A* and *B*). This dynamic *Staphylococcus* pattern is recapitulated by the expression of the 258 IR, DR, and WR genes most positively correlated with *Staphylococcus* (Fig. 5 *C–F*; Table S4). This correlation is underscored by our observation that the majority of biological processes most significantly enriched in genes highly correlated with *Staphylococcus* abundance are processes relevant to the cutaneous host defense response (Table S5).

Discussion

Our findings have shown that skin in a diabetic mouse model was characterized by a selective shift in colonizing bacteria and was accompanied by a transcriptional profile that suggests mobilized defense and immune responses. After wounding, we observed a selective microbial shift of Firmicutes species (including *Staphylococcus* and *Aerococcus*) longitudinally through day 28 in tandem with a prolonged immune response in diabetic wounds. The selective *Staphylococcal* shift correlates specifically with aberrantly expressed genes related to the cutaneous defense response. Thus, we demonstrated that the colonizing microbiota was intertwined with the skin's response to injury.

Staphylococcus has been associated with impaired wound healing in clinical and laboratory models. *Staphylococcus* is readily identified by culture in all types of leg ulcers (26–28). In normal C57Bl6/J mice, colonization and biofilm formation by either *S. aureus* or *S. epidermidis* impaired wound reepithelialization (29). In a model of *S. aureus* infection, db/db mice developed chronic infections along with an inflammatory response characterized by defective phagocytic function, suggesting an aberrant innate immune response in the diabetic host (30). We have extended these observations by surveying the microbiota in a less-biased genomic manner, identifying altered bacterial community structure in the diabetic wound, including a shift in *Staphylococcus* relative abundance.

Previous work has demonstrated that commensal microbiota can influence the cutaneous host–defense response (31). We now show, on a global level, that the skin and wound microbiome correlates with the transcriptional signature of the cutaneous defense response in db/db mice. An aberrant immune response, including chronic inflammation, is a well-established hallmark of impaired diabetic wound healing (10–13). Our transcriptional dataset suggests elements of inflammation and a mobilized defense response before wounding. This feature could in part be due to increased bacteria load and/or altered bacterial populations such as we observe on db/db skin. Once wounding occurs, bacterial populations could be responsible for the exacerbation and prolongation of the immune response that we observe, further impairing healing through the recruitment of macrophages, monocytes, and polymorphonuclear leukocytes and resulting in damage due to ROS production. Although we can only predict that prolonged gene expression of particular immune effectors is indicative of a bacterial-specific response, our results may provide a foundation for future
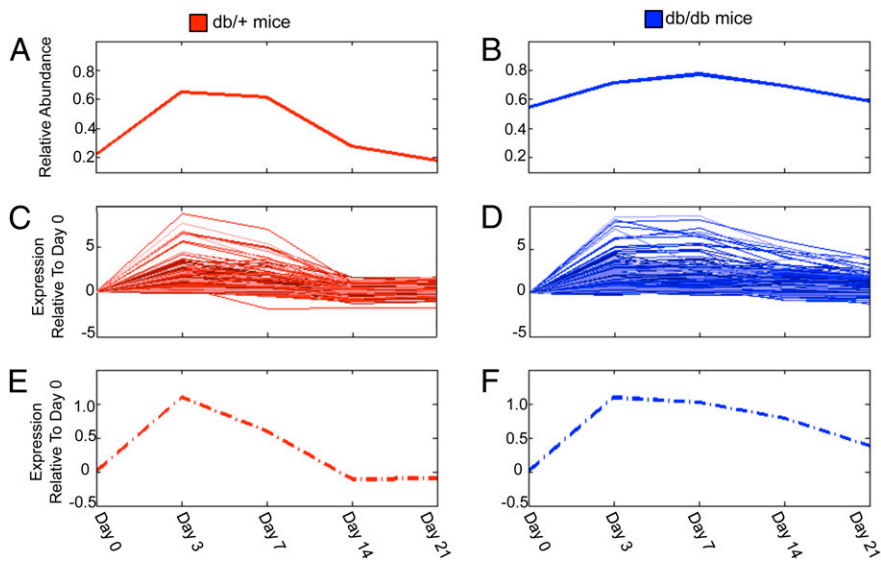
Fig. 5. Positive correlation between expression of cutaneous host–defense genes and *Staphylococcus* relative abundance. The relative abundance of *Staphylococcus* at the wound site in db/+ (*A*, red) and db/db (*B*, blue) mice are shown during the wound time course. Using Gene Set Enrichment Analysis, the GO biological processes IR, DR, and WR are significantly enriched among those genes whose expression is most positively correlated with *Staphylococcus* abundance. Leading edge subset analysis was used to extract the 258 genes contributing to this enrichment. The longitudinal expression of these 258 genes is shown for db/+ (*C*, red) and db/db (*D*, blue) mice. The median expression of these genes is shown for db/+ (*E*, red) and db/db (*F*, blue) mice.

interrogation of specific innate immune pathways in the pathophysiology of impaired wound healing. For example, aberrant of expression of TLRs 1 and 2 suggests a mobilized response to Gram-positive bacteria, whereas TLR4 activation suggests a response specific to Gram-negative bacteria in our particular dataset.

One of the major objectives of the National Institutes of Health Roadmap Human Microbiome Project is to determine whether changes in the microbiome are related to human health and disease, with an ultimate goal of improving human health through monitoring or manipulation of the microbiome (32). These findings support the widely appreciated clinical observation that microbial colonization of diabetic wounds contributes to impaired wound healing. Moreover, this molecular discovery that diabetic mouse skin harbors a quantitatively and qualitatively distinct microbial population, along with a distinct host gene expression profile, are important contributions to our understanding of microbial–skin interactions in diabetic ulcers. Microbial or transcriptional signatures such as these could potentially act as "biomarkers" to identify clinical populations at risk for chronic wounds, potentially leading to improved preventive and therapeutic measures. One such treatment modality directed toward minimizing complications of bacterial infections is the use of dilute bleach baths for patients with moderate to severe atopic dermatitis (33). This simple measure to decrease overall bacterial load is preferable to the long-term use of antibiotics that leads to antibiotic-resistant bacteria. Normalization of the wound microbiome, through inhibition of pathogenic bacteria or promotion of symbiotic bacteria, would provide a low-cost, noninvasive target for the management of nonhealing diabetic wounds.

Wound healing is a highly relevant model to dissect the interaction of two key components of the genomic landscape, the microbiome and the host transcriptional response. Although other factors such as neuropathy and vasculopathy play a key role in initial wounding and impaired wound healing, the microbiome and the innate immune system are additional potential targets for preventive and therapeutic intervention. Our work shows that two global genomic datasets, microbiome diversity and gene expression, can be integrated and correlated to gain a better understanding of the dynamics governing wound healing in a diabetic model.

Materials and Methods

Animal Model. All experiments were approved and performed under the guidelines of the National Human Genome Research Institute Animal Care and Use Committee. Ten each of 12-wk-old female mice homozygous for the *Lepr*^db^ mutation (db/db) and age-matched female nondiabetic heterozygous littermates (db/+) were used in these experiments (Jackson Laboratory; BKS. Cg-Dock$^{7m+/+}$Lepr^{db}/J, strain No. 000642). Mice were housed individually beginning 2 wk before the start of the time course. After anesthesia with inhaled isofluorane, a dorsal patch of skin was shaved. The following day, an area of 4 cm^2 was swabbed with a cotton-tipped applicator (Medline Industries) soaked in enzymatic lysis buffer (20 mM Tris at pH 8, 2 mM EDTA, and 1.2% Triton X-100). A 6-mm full thickness excisional wound was created by using a dermal punch biopsy tool (Miltex). Swabs were collected from wounds with cotton tipped applicators moistened in enzymatic lysis butter. For microarray experiments, animals were prepared as above, but the wound was excised and stored in RNAlater (Ambion).

DNA Extraction. Bacterial swabs were incubated in enzymatic lysis buffer and lysozyme (20 mg/mL) for 30 min at 37 °C. The standard protocol for the PureLink Genomic DNA kit (Invitrogen) was followed for all subsequent steps.

Quantification of Total Bacteria. Quantification is as described (14).

PCR Amplification, Cloning, and Sequencing of 16S rRNA Genes. rRNA genes (16S) were amplified from purified genomic DNA by using primers 27F (5'-AGRGTTTGATCMTGGCTCAG-3') and 1492R (5'-TACGGYTACCTTGTTAYGA-CTT-3'). PCR, cloning, and sequencing were performed as described (7). Sequence assembly, alignment, chimera elimination, OTU clustering, and diversity estimation were performed as described (7). Sequence details are in *SI Materials and Methods*.

RNA Preparation and Array Hybridization. Total RNA was extracted from 2 mm of wound edge tissue and wound bed (if present) stored in RNAlater (Ambion) at days 0, 3, 7, 14, and 21. RNA extraction was performed by using the RNeasy kit and Tissue Lyser (Qiagen) according to manufacturers' protocol. Microarray chips were hybridized to independent samples for db/db (n = 4) and db/+ (n = 4) wounds at each time point. RNA quality was verified on a 2100 Bioanalyzer (Agilent). CRNA was generated and labeled according to manufacturer's instructions by using the Illumina TotalPrep RNA Amplification Kit (Ambion) and hybridized to GeneChip 430 2.0 mouse arrays (Affymetrix). Arrays were washed, stained, and scanned by NHGRI Microarray Core in one batch on the Complete GeneChip Instrument System (Affymetrix) according to manufacturer's protocol. GCOS (GeneChip Operating Software; Affymetrix) was used for data acquisition and image processing. Raw data were processed by using Robust Multichip Average (RMA) method (35).

Microarray Expression Analysis. Microarray pairwise comparisons were performed in GeneSifter (VizX Labs) by using a Student's *t* test cutoff >1.5-fold change and adjusted *P* value of 0.05 after Benjamini–Hochberg correction. Hierarchical clustering of samples was performed by using the Euclidean distance metric and clustering by average linkage. GO and KEGG pathway enrichment analysis was performed by using the publicly available DAVID Resource (http://david.abcc.ncifcrf.gov/). *P* values reported are EASE scores adjusted for multiple comparisons by Benjamini–Hochberg correction.

Clustering of Time Course Expression Data. The Short Time-series Expression Miner (STEM) (18) version 1.3.6 was downloaded from http://www.cs.cmu.edu/~jernst/stem. The STEM clustering method was applied by using a maximum of 50 model profiles and a maximum unit change between time points of 2. A false discovery rate of 0.05 was used to identify significant expression profiles. GO term enrichment significance values were corrected by using $n = 500$ randomizations. Comparison of the two datasets (db/db and db/+) was performed by using a maximum uncorrected intersection P value of 0.005.

Gene Set Enrichment Analysis. Gene set enrichment analysis (GSEA) was implemented as described and performed independently for each of the 11 most abundant genera (21). Details of implementation and analysis can be found in *SI Materials and Methods*.

Correlation of Gene Expression and Microbiome Data. The nonparametric Spearman rank correlation was used to quantify the association between the expression time course of each gene and the time course of each of the 11 most abundant genera. To increase power, the db/+ and db/db time-courses were considered together for calculation of each correlation. P values reported are adjusted by Benjamini–Hochberg correction.

Statistical Analysis. The nonparametric Mann–Whitney u test was used to compare bacterial loads and bacterial relative abundance between db/db and db/+ groups ($n = 10$ each). Wound sizes and diversity indices were compared by using the Welch's t test so that no assumptions were made concerning population variances. Microarray statistical analysis is described in the corresponding methods sections.

1. Huang ES, Basu A, O'Grady M, Capretta JC (2009) Projecting the future diabetes population size and related costs for the U.S. *Diabetes Care* 32:2225–2229.
2. Harrington C, Zagari MJ, Corea J, Klitenic J (2000) A cost analysis of diabetic lower-extremity ulcers. *Diabetes Care* 23:1333–1338.
3. Falanga V (2005) Wound healing and its impairment in the diabetic foot. *Lancet* 366:1736–1743.
4. Gardner SE, Frantz RA (2008) Wound bioburden and infection-related complications in diabetic foot ulcers. *Biol Res Nurs* 10:44–53.
5. Bowler PG, Duerden BI, Armstrong DG (2001) Wound microbiology and associated approaches to wound management. *Clin Microbiol Rev* 14:244–269.
6. Dunbar J, Barns SM, Ticknor LO, Kuske CR (2002) Empirical and theoretical bacterial diversity in four Arizona soils. *Appl Environ Microbiol* 68:3035–3045.
7. Grice EA, et al.; NISC Comparative Sequencing Program (2009) Topographical and temporal diversity of the human skin microbiome. *Science* 324:1190–1192.
8. Blaser MJ (2006) Who are we? Indigenous microbes and the ecology of human diseases. *EMBO Rep* 7:956–960.
9. Barker JN, Mitra RS, Griffiths CE, Dixit VM, Nickoloff BJ (1991) Keratinocytes as initiators of inflammation. *Lancet* 337:211–214.
10. Zykova SN, et al. (2000) Altered cytokine and nitric oxide secretion in vitro by macrophages from diabetic type II-like db/db mice. *Diabetes* 49:1451–1458.
11. Fahey TJ, 3rd, et al. (1991) Diabetes impairs the late inflammatory response to wound healing. *J Surg Res* 50:308–313.
12. Calhoun JH, Overgaard KA, Stevens CM, Dowling JP, Mader JT (2002) Diabetic foot ulcers and infections: Current concepts. *Adv Skin Wound Care* 15:31–42; quiz 44–45.
13. Naghibi M, et al. (1987) The effect of diabetes mellitus on chemotactic and bactericidal activity of human polymorphonuclear leukocytes. *Diabetes Res Clin Pract* 4:27–35.
14. Chen H, et al. (1996) Evidence that the diabetes gene encodes the leptin receptor: Identification of a mutation in the leptin receptor gene in db/db mice. *Cell* 84:491–495.
15. DiPietro LA, Burns AL (2003) *Wound Healing: Methods and Protocols* (Humana Press, Totowa, NH).
16. Michaels J, 5th, et al. (2007) db/db mice exhibit severe wound-healing impairments compared with other murine diabetic strains in a silicone-splinted excisional wound model. *Wound Repair Regen* 15:665–670.
17. Castillo M, et al. (2006) Quantification of total bacteria, enterobacteria and lactobacilli populations in pig digesta by real-time PCR. *Vet Microbiol* 114:165–170.
18. Grice EA, et al.; NISC Comparative Sequencing Program (2008) A diversity profile of the human skin microbiota. *Genome Res* 18:1043–1050.
19. Cole JR, et al. (2007) The ribosomal database project (RDP-II): Introducing myRDP space and quality controlled public data. *Nucleic Acids Res* 35(Database issue):D169–D172.
20. Schloss PD, Handelsman J (2005) Introducing DOTUR, a computer program for defining operational taxonomic units and estimating species richness. *Appl Environ Microbiol* 71:1501–1506.
21. Ashburner M, et al.; The Gene Ontology Consortium (2000) Gene ontology: Tool for the unification of biology. *Nat Genet* 25:25–29.
22. Ernst J, Bar-Joseph Z (2006) STEM: A tool for the analysis of short time series gene expression data. *BMC Bioinformatics* 7:191.
23. Wetzler C, Kämpfer H, Stallmeyer B, Pfeilschifter J, Frank S (2000) Large and sustained induction of chemokines during impaired wound healing in the genetically diabetic mouse: Prolonged persistence of neutrophils and macrophages during the late phase of repair. *J Invest Dermatol* 115:245–253.
24. Eming SA, Krieg T, Davidson JM (2007) Inflammation in wound repair: Molecular and cellular mechanisms. *J Invest Dermatol* 127:514–525.
25. Subramanian A, et al. (2005) Gene set enrichment analysis: A knowledge-based approach for interpreting genome-wide expression profiles. *Proc Natl Acad Sci USA* 102:15545–15550.
26. Bowler PG, Davies BJ (1999) The microbiology of infected and noninfected leg ulcers. *Int J Dermatol* 38:573–578.
27. Citron DM, Goldstein EJ, Merriam CV, Lipsky BA, Abramson MA (2007) Bacteriology of moderate-to-severe diabetic foot infections and in vitro activity of antimicrobial agents. *J Clin Microbiol* 45:2819–2828.
28. Sopata M, Luczak J, Ciupinska M (2002) Effect of bacteriological status on pressure ulcer healing in patients with advanced cancer. *J Wound Care* 11:107–110.
29. Schierle CF, De la Garza M, Mustoe TA, Galiano RD (2009) Staphylococcal biofilms impair wound healing by delaying reepithelialization in a murine cutaneous wound model. *Wound Repair Regen* 17:354–359.
30. Park S, Rich J, Hanses F, Lee JC (2009) Defects in innate immunity predispose C57BL/6J-Leprdb/Leprdb mice to infection by Staphylococcus aureus. *Infect Immun* 77:1008–1014.
31. Lai Y, et al. (2009) Commensal bacteria regulate Toll-like receptor 3-dependent inflammation after skin injury. *Nat Med* 15:1377–1382.
32. Peterson J, et al.; NIH HMP Working Group (2009) The NIH Human Microbiome Project. *Genome Res* 19:2317–2323.
33. Huang JT, Abrams M, Tlougan B, Rademaker A, Paller AS (2009) Treatment of Staphylococcus aureus colonization in atopic dermatitis decreases disease severity. *Pediatrics* 123:e808–e814.